



# Glutamine regulates mitochondrial uncoupling protein 2 to promote glutaminolysis in neuroblastoma cells

Anne Rupprecht<sup>a,b,\*</sup>, Rudolf Moldzio<sup>c</sup>, Bernadette Mödl<sup>a</sup>, Elena E. Pohl<sup>a,\*</sup>

<sup>a</sup> Institute of Physiology, Pathophysiology and Biophysics, Department of Biomedical Sciences, University of Veterinary Medicine, Vienna, Austria

<sup>b</sup> Institute of Pharmacology and Toxicology, Rostock University Medical Center, Germany

<sup>c</sup> Institute of Medical Biochemistry, Department of Biomedical Sciences, University of Veterinary Medicine, Vienna, Austria

## ABSTRACT

Mitochondrial uncoupling protein 2 (UCP2) is highly abundant in rapidly proliferating cells that utilize aerobic glycolysis, such as stem cells, cancer cells, and cells of the immune system. However, the function of UCP2 has been a longstanding conundrum. Considering the strict regulation and unusually short life time of the protein, we propose that UCP2 acts as a “signaling protein” under nutrient shortage in cancer cells. We reveal that glutamine shortage induces the rapid and reversible downregulation of UCP2, decrease of the metabolic activity and proliferation of neuroblastoma cells, that are regulated by glutamine per se but not by glutamine metabolism. Our findings indicate a very rapid (within 1 h) metabolic adaptation that allows the cell to survive by either shifting its metabolism to the use of the alternative fuel glutamine or going into a reversible, more quiescent state. The results imply that UCP2 facilitates glutamine utilization as an energetic fuel source, thereby providing metabolic flexibility during glucose shortage. The targeting UCP2 by drugs to intervene with cancer cell metabolism may represent a new strategy for treatment of cancers resistant to other therapies.

## 1. Introduction

Rapidly proliferating cells share characteristic metabolism, known as aerobic glycolysis first described for cancer cells [1–3]. Aerobic glycolysis is characterized by high glucose consumption. Most pyruvate, which is raised from glycolysis even in the presence of oxygen, is converted into lactate and secreted out of cells. Only small amounts of pyruvate enter mitochondria, fill the citrate acid cycle (CAC), and drive oxidative phosphorylation. High glutamine usage is another hallmark of the metabolism of rapidly proliferating cells and it becomes a most prominent target in cancer treatment [4]. Glutamine fills the CAC and drives mitochondrial metabolism for cellular precursor synthesis supporting high proliferation rate [5]. It can act as an alternative energy fuel source in mitochondrial oxidative phosphorylation during glucose shortage and even contribute to the formation of pyruvate via malate [5,6]. Such an adaptive metabolic mechanism confers high metabolic flexibility to cancer cells. These less understood mechanisms adjust cellular metabolism in situations like nutrient limitation that take place during tumor growth [7,8].

Our group and others have recently shown that mitochondrial uncoupling protein 2 (UCP2) is highly abundant in cancer cells [9–11]. UCP2 belongs to the mitochondrial anion carrier superfamily and is

assumed to be located in the inner mitochondrial membrane similar to other UCPs [12]. It has 57% homology to UCP1, the mediator of non-shivering thermogenesis in brown adipose tissue. The molecular function of UCP2 is still a matter of debate. We and others have demonstrated that UCP2 transports protons at a rate of 4.5/s, which is similar to UCP1 and UCP3 [13–15]. It has been suggested for a long time, that UCP2 acts as a mild uncoupler in the reduction of oxidative stress [16,17]. This function that has been generally proposed for all UCPs [18] is in conflict with the new emerging concept of UCP2 tissue distribution, implying that UCP2 expression is only confined to cells that rely on aerobic glycolysis, including cancer cells [9,19–21]. The involvement of UCP2 in metabolism is consistent with its recently proposed function to transport C4-metabolites out of mitochondria facilitating the CAC and regulating thereby the metabolism and ROS [22]. Nonetheless, the reports about UCP2's role in cancer cells are contradictory. On the one side, UCP2 was described to induce aerobic glycolysis [23–25] and even inhibit pyruvate entry into the mitochondria [20]. On the other side, UCP2 was shown to support oxidative phosphorylation [21,22,26]. The conclusions of these studies were based on the knockout, knockdown, or overexpression of UCP2 and did not consider the unusually short lifetime of UCP2 [27], which rather indicates the rapid, transient function of UCP2.

**Abbreviations:** Asp, aspartate; CAC, citrate acid cycle; CYC, cycloheximide; ECAR, extracellular acidification rate; GAPDH, glyceraldehyde 3-phosphate dehydrogenase; Glc, glucose; Gln, glutamine; Glu, glutamic acid; OCR, oxygen consumption rate; Pyr, pyruvate; SDHA, succinate dehydrogenase subunit A; UCP, uncoupling protein; uORF, upstream open reading frame; VDAC, voltage dependent anion channel

\* Corresponding authors.

E-mail addresses: [anne.rupprecht@med.uni-rostock.de](mailto:anne.rupprecht@med.uni-rostock.de) (A. Rupprecht), [elena.pohl@vetmeduni.ac.at](mailto:elena.pohl@vetmeduni.ac.at) (E.E. Pohl).

<https://doi.org/10.1016/j.bbambio.2019.03.006>

Received 6 August 2018; Received in revised form 30 December 2018; Accepted 14 March 2019

Available online 15 March 2019

0005-2728/ © 2019 Published by Elsevier B.V.

Here we propose that UCP2 is involved in the metabolic adaptation of cancer cells. In particular, we hypothesize that under conditions of nutrient deprivation, UCP2 ensures the high metabolic flexibility of cells. To test this hypothesis, we analysed UCP2 expression and cellular metabolism during a shortage of glucose and glutamine in neuroblastoma cells. Based on the strong correlation between UCP2 abundance and nutrient availability, we describe a new metabolic adaptation mechanism that involves UCP2.

## 2. Results

### 2.1. UCP2 is upregulated during glucose deprivation

To evaluate the putative involvement of UCP2 in the adaptation process during glucose shortage we analyzed the murine neuroblastoma cell line N18TG2, which has a high level of UCP2 protein expression [9]. First, we incubated the cells for 24 h with (i) 5.2 mM glucose, which mimics physiological concentration of glucose in blood, (ii) 2.6 mM or (iii) 1.3 mM, reflecting low glucose concentrations. The concentration of other nutrients was kept constant. Fig. 1, A demonstrates that UCP2 levels were significantly increased at 2.6 mM and 1.3 mM of glucose. Assuming that UCP2 protein acts very fast, we analyzed its expression at different incubation times (Fig. 1, B). The immunoblot analysis showed a rapid increase in UCP2 levels within the

first 4 h, following by renewed slow upregulation after 16 h. The increase in UCP2 abundance cannot be interpreted as an increase in the number of mitochondria, because we did not detect changes in the levels of other mitochondrial membrane proteins, such as voltage-dependent anion channel (VDAC) and succinate dehydrogenase subunit A (SDHA) (Fig. 1, A and B). The expression of the housekeeping gene glyceraldehyde 3-phosphate dehydrogenase (GAPDH) and cytoskeleton protein  $\beta$ -actin showed no alteration under these conditions. The absence of significant changes in UCP2 and GAPDH mRNA levels (Fig. 1, C and D) indicated the regulation of UCP2 only at the protein level.

### 2.2. UCP2 is downregulated during glutamine shortage

Glutamine is the second important nutrient in rapidly proliferating cells [28]. To investigate the expression of UCP2 under glutamine shortage, we compared UCP2 abundance in N18TG2 cells under high concentration of glutamine (3.8 mM) with concentrations of glutamine ranging from 1.9 mM to 0.4 mM in the presence of all other nutrients after 24 h of incubation (Fig. 2, A). The immunoblot analysis demonstrated a significant decrease in UCP2 protein levels, which correlated to the glutamine amount in the growth medium. The immunoblot analysis of N18TG2 cells incubated with 0.4 mM glutamine at different incubation times revealed a strong downregulation of UCP2 within the first 4 h (Fig. 2, B). Neither of the above mentioned mitochondrial or

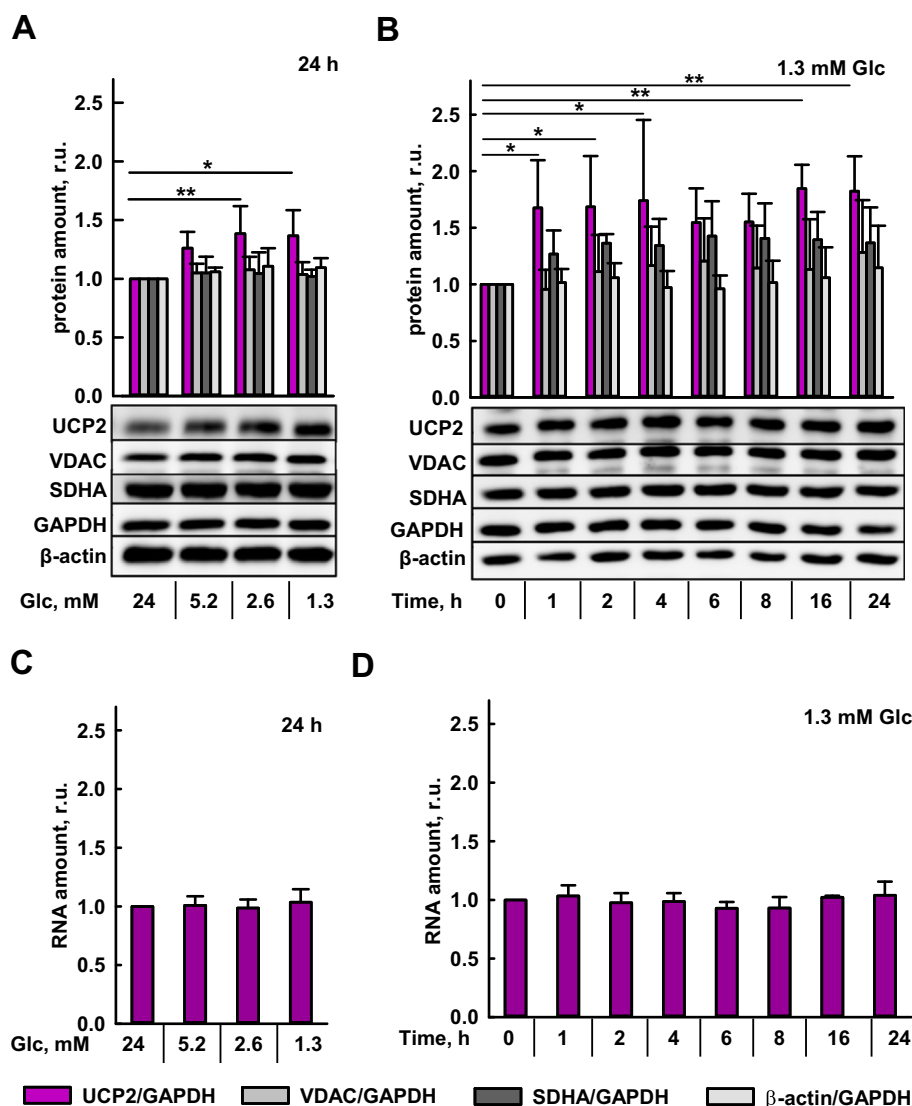
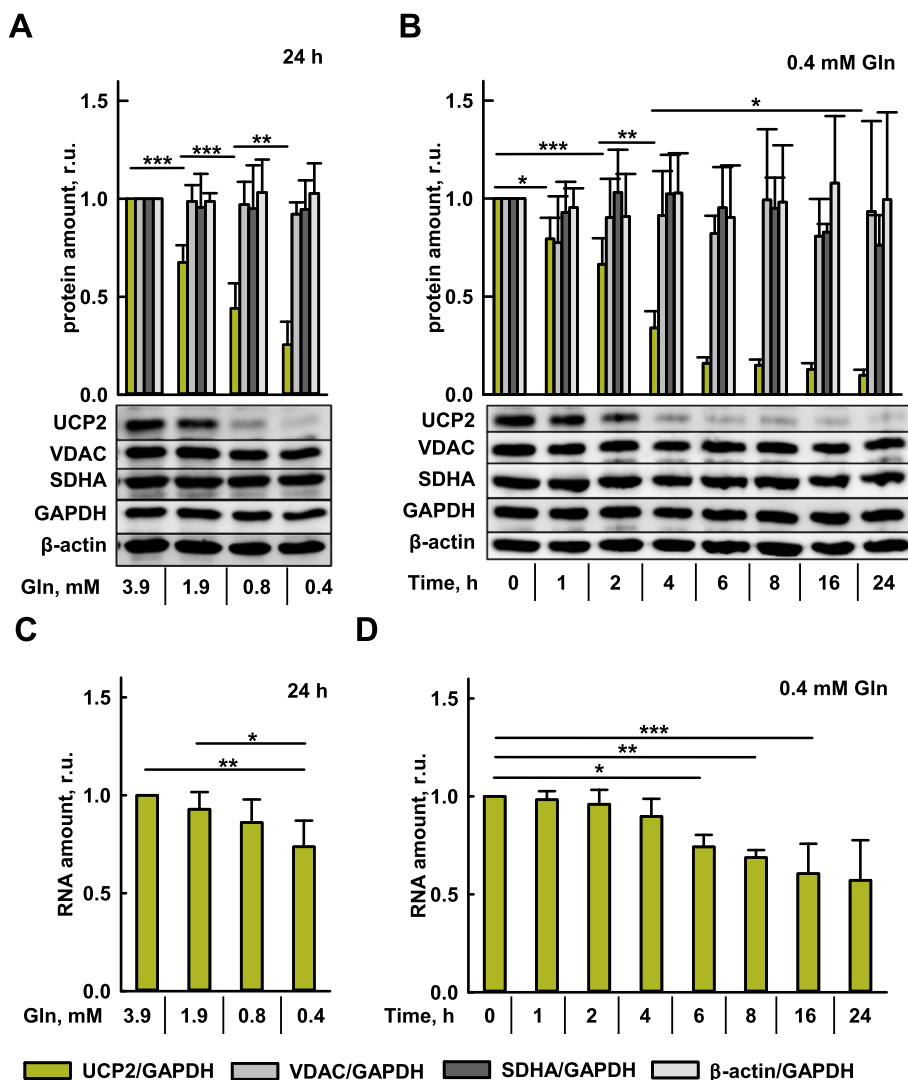


Fig. 1. UCP2 is upregulated during glucose deprivation

Immunoblot analysis was performed with total cellular protein isolated from N18TG2 cells using indicated antibodies. Cells were grown for 24 h in media with different glucose (Glc) concentrations (A) or in medium containing 1.3 mM Glc for indicated incubation time (B). Figures show the quantitative analysis of five (A) or six (B) independent experiments and representative immunoblots. Protein amount is presented as a ratio between the band intensities of UCP2 and GAPDH and normalized to the band intensity of control cells grown in medium containing 24 mM Glc. Quantitative PCR of *ucp2* is presented as ratio to *gapdh* normalized to the control from three independent experiments. RNA was isolated from N18TG2 cells grown for 24 h at different Glc concentrations (C) or in medium containing 1.3 mM Glc for different incubation time (D).



**Fig. 2.** UCP2 down-regulation during glutamine shortage.

Total cellular protein from N18TG2 cells was analyzed by immunoblot with the indicated antibodies. Cells were grown for 24 h at different glutamine (Gln) concentrations (A) or in medium containing 0.4 mM Gln for indicated incubation time (B). Quantitative analysis was made from five (A) or three (B) independent experiments and calculated as a band intensities ratio (UCP2 to GAPDH and normalized to the control). One representative immunoblot is shown. Isolated RNA from N18TG2 cells was analyzed by quantitative PCR for *ucp2* and *gapdh*. Cells were grown at different Gln concentrations for 24 h (C) or in medium containing 0.4 mM Gln for indicated incubation time (D). Graph shows *ucp2* in relation to *gapdh* normalized to the control.

cytosolic proteins showed an expression regulation due to glutamine shortage under these conditions (Fig. 2, A and B). The quantitative RNA analysis that was performed in parallel showed a delayed decrease in *ucp2* levels only at the glutamine concentration of 0.4 mM (Fig. 2, C) after an incubation time of at least 6 h (Fig. 2, D). This discrepancy between UCP2 protein and mRNA levels indicates two different steps of UCP2 regulation: rapid regulation at the protein level and delayed regulation of the gene.

### 2.3. Glutamine shortage shifts the cells to a reversible, more quiescent metabolic state

To analyze the impact of glucose and glutamine shortage on the metabolic activity of N18TG2 cells in parallel to the affected UCP2 levels we determined the extracellular acidification rate (ECAR) (Fig. 3, A) and oxygen consumption rate (OCR) (Fig. 3, B) of cells that were incubated 1 or 4 h under glucose or glutamine shortage in comparison to cells that were grown in a medium with high amounts of nutrients (control). As expected, the ECAR was reduced within 1 h in the absence of glucose. Surprisingly, 1.3 mM glucose kept a quite high level of ECAR up to 4 h of incubation. Incubation with the full amount of glucose (24 mM) swiftly recovered the ECAR after 3 h incubation with 1.3 mM glucose. The OCR of neuroblastoma cells during glucose shortage was similar to cells that were grown under a full glucose supply (Fig. 3, B). This can be interpreted as (i) absence of glucose participation in

oxidative phosphorylation or (ii) the utilization of an alternative fuel source to support mitochondrial oxidation during glucose shortage. Extracellular glutamine determination revealed an increased glutamine consumption in cells that were grown 4 h under glucose shortage in contrast to control cells (Supplementary Materials, Fig. S3). On the contrary, glutamine shortage had a drastic effect on the OCR. The OCR was reduced within 1 h and further decreased after 4 h (Fig. 3, B). Surprisingly, the ECAR also decreased during glutamine shortage after 4 h incubation (Fig. 3, A). Addition of media containing a full supply of glutamine recovered both the OCR and the ECAR. The metabolic profile revealed that the cells shifted more to oxidative metabolism under glucose shortage, whereas under glutamine shortage they shifted from a high energetic state to a more quiescent state (Fig. 3, C). This shift was rapidly reversed by reinstating glutamine availability. The application of both oligomycin and FCCP also revealed that the cells retained their spare capacity during glutamine shortage. That is, cells were still able to increase their metabolic activity when suddenly challenged by FCCP (Fig. 3, D and E). It indicates that the regulation due to glutamine shortage occurs upstream of mitochondrial energy metabolism and results in a lower energy requirement due to attenuation of the energy-consuming processes, such as DNA/RNA synthesis, protein synthesis and proliferation (for review, see [29]). Interestingly, proton leak (as difference between OCR in the presence of oligomycin and rotenone/antimycin) markedly decreased during glutamine shortage (Fig. 3, D and E). It correlated with the UCP2 levels (Fig. 2) and implies that UCP2

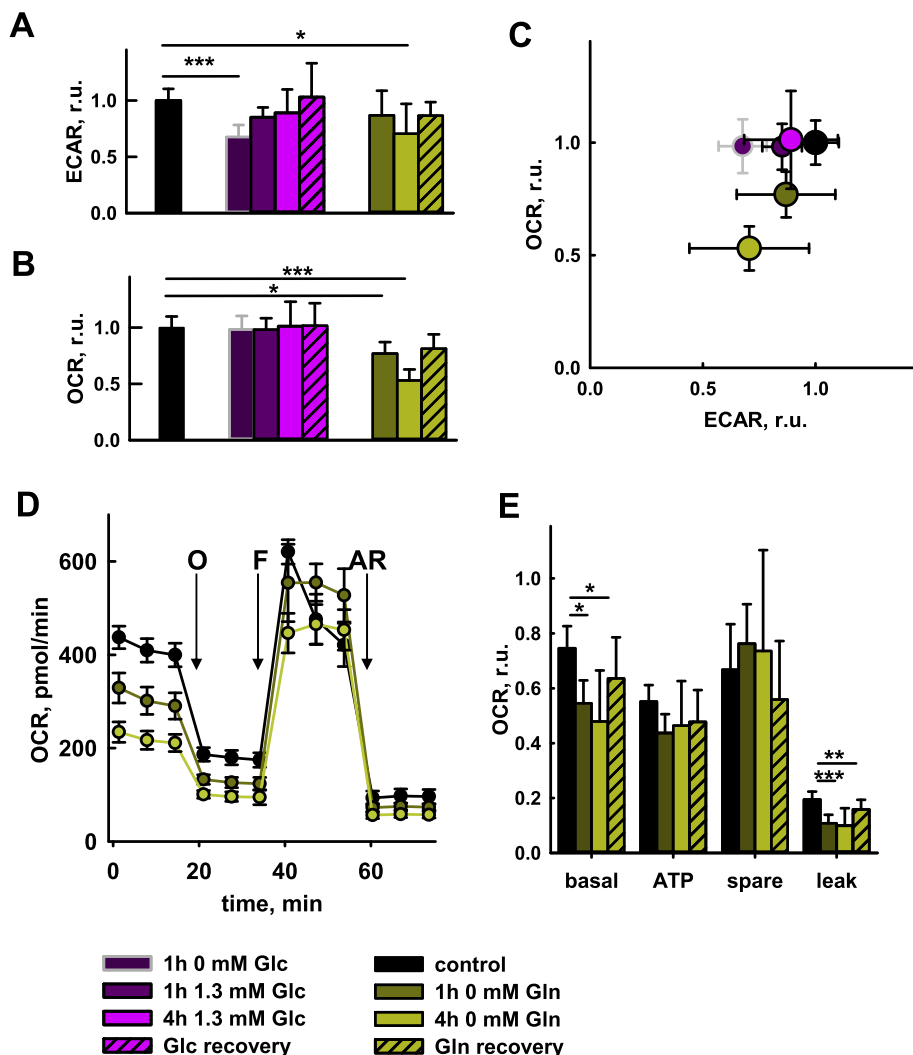


**Fig. 3.** Glutamine shortage induces a metabolically reversible quiescence.

Extracellular flux analysis of N18TG2 cells during Glc or Gln shortage (A–E): extracellular acidification rate (ECAR; A) and oxygen consumption rate (OCR; B) determined from 3 to 6 independent experiments and normalized to the mean of the control of each experiment. The mean and SD are calculated from all experiments using random number generation to create 1000 values for each single experiment. The graph (C) demonstrates an energetic plot of the ECAR and OCR data from (A–B). (D–E) A representative experiment and the quantitative analysis of 3–6 independent “Mito stress test” - experiments (E) during Gln shortage and recovery. O, oligomycin; F, FCCP; AR, antimycin/rotenone ratio. OCR of basal capacity, ATP production, spare capacity and proton leak for each group were normalized to the OCR of the mean of the control of the respective experiment. All data were summarized to a mean values ± SD using random number generator.

increases basal proton leak. Interestingly, no increased proton leak was measured during glucose shortage (Supplementary Materials, Fig. S4).

**2.4. Nutrient shortage reduces cell proliferation**

We then tested whether a reduced proliferation might be the upstream regulation step of glutamine shortage. Fig. 4 shows that whereas cells had a doubling time of 22.5 h under control conditions, glucose and even more the glutamine shortage led to a reduction in the proliferation displaying a four-fold increase in cell number doubling time. However, within the first 24 h, cell proliferation was not visibly affected.

**2.5. Inhibition of mitochondrial nutrient usage had minimal effect compared to nutrient shortage**

To evaluate the role of mitochondrial metabolism in the adaptation to nutrient shortage we tested, how the inhibition of the mitochondrial oxidation pathways affects metabolic activity. Surprisingly, application of the glutaminase inhibitor BPTES under full nutrient conditions only moderately reduced the OCR, accompanied by a slight increase in the ECAR (Fig. 5, A) in comparison to the magnitude of glutamine shortage effect (Fig. 3, B). This indicates that the lower energetic state that was induced by glutamine shortage was not due to reduced mitochondrial glutamine oxidation. The inhibition of mitochondrial pyruvate entry by UK-5099 (Fig. 5, A) caused a significant reduction in OCR, which is in

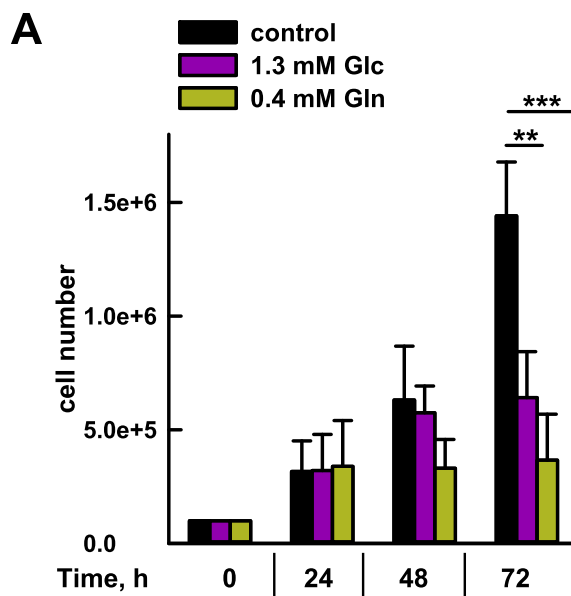


**Fig. 4.** Nutrient shortage reduces the proliferation. Cell doubling time analysis of N18TG2 cells was performed during Gln or Glc shortage. Data represent mean values ± SD from at least three independent experiments.

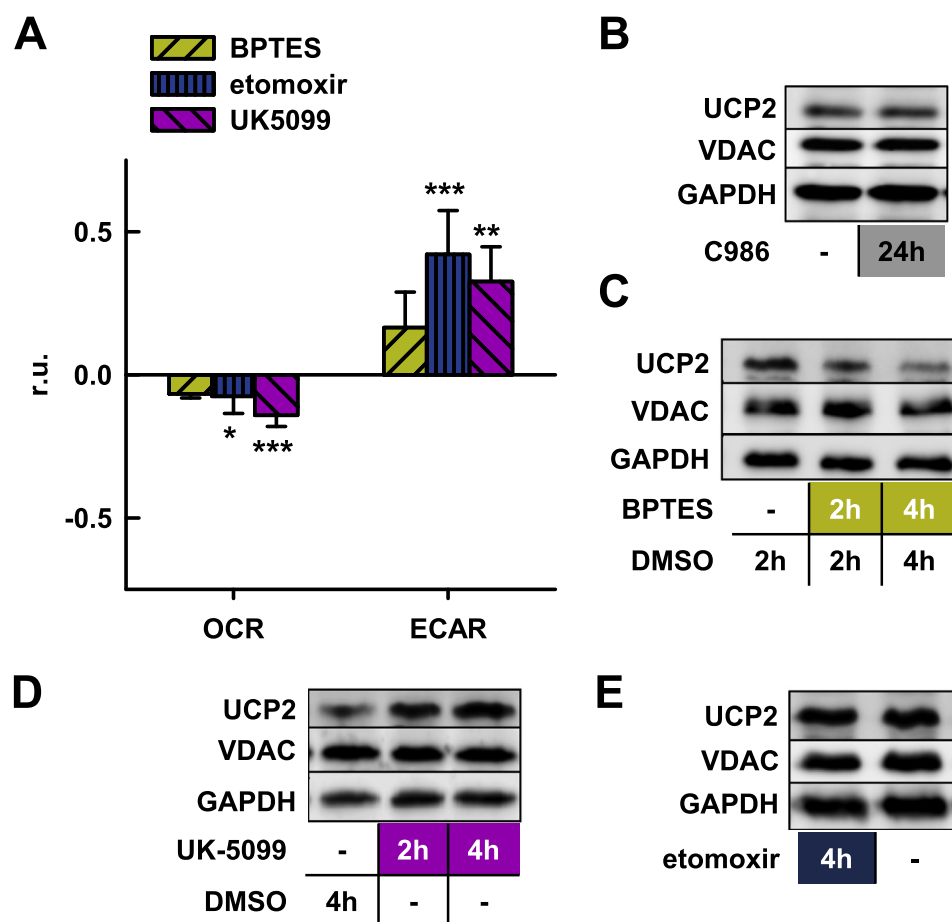


**Fig. 5.** Effect of nutrient usage inhibitors on cell metabolic parameters and UCP2 expression. Change of OCR and ECAR within 1 h after the addition of inhibitors was calculated to OCR and ECAR values prior addition. 3  $\mu$ M BPTES, 40  $\mu$ M etomoxir, or 2  $\mu$ M UK-5099 were added. Data are mean values  $\pm$  SD from 4 independent experiments (A). Representative immunoblots of total cellular protein from N18TG2 cells incubated in the presence of 5  $\mu$ M C968 (B), 3  $\mu$ M BPTES (C), 10  $\mu$ M UK-5099 (D) or 50  $\mu$ M etomoxir (E).

contrast to the constant OCR during glucose deficiency (Fig. 3, B). Also the inhibition of carnitine palmitoyltransferase-1, component of the fatty acid oxidation cascade, by etomoxir reduced the OCR. The inhibition of these two mitochondrial oxidation pathways led to a significant increase in the ECAR, indicating compensation by glycolysis (shift to a glycolytic metabolism).

Next we tested how the inhibition of these mitochondrial oxidation pathways alters the expression of UCP2. Using the glutaminase inhibitor C968 at different concentrations and with different incubation times, we observed no effect on UCP2 expression (Fig. 5, B). In contrast, the addition of BPTES led to a reduction of UCP2 within 4 h (Fig. 5, C). Both inhibitors act differently [30]. C968 was shown to prevent glutaminase activation, whereas BPTES inhibits its active form. Moreover, it was shown before that glutaminase inhibition by BPTES impairs mTOR activation even in the presence of glutamine [31]. The lack of mTOR activation leads to a general reduction of protein translation [32,33], which affects the short-living UCP2 in the first line. However, the decrease of UCP2 levels due to glutamine shortage (Fig. 2, B, 2 and 4 h) was still stronger than due to BPTES administration. Therefore, we cannot conclude that the inhibition of glutamine metabolism regulates UCP2 levels.

Notably, inhibition of the mitochondrial pyruvate uniporter led to an increase in UCP2 expression (Fig. 5, D), which was comparable to the effect of glucose shortage (Fig. 1, B). A reduced pyruvate entry in mitochondria might be a signal to upregulate UCP2. In comparison, impairment of the FA oxidation metabolism after the application of etomoxir had no impact on UCP2 expression (Fig. 5, E). In this case, glucose metabolism may compensate for the reduced fatty acid oxidation. Our data indicate that metabolic adaptation during nutrient shortage occurs upstream of mitochondrial metabolism.

## 2.6. Glutamine availability is a driving force of UCP2 expression

To investigate whether the mitochondrial entry of pyruvate raised from glycolysis causes the UCP2 upregulation during glucose shortage, we grew cells without pyruvate. We combined a high glucose concentration (24 mM) or a low glucose concentration (1.3 mM) with or without a high pyruvate concentration (2 mM) (Fig. 6, A). The immunoblot analysis revealed that even pyruvate absence induced some increase in UCP2 expression. Notably, the combination of low glucose and a lack of pyruvate resulted in the highest UCP2 expression levels. The result indicates that the absence of pyruvate to fill the CAC and not the reduced cytosolic glycolysis induces UCP2 upregulation. In contrast, glutamine shortage led to a similar UCP2 drop regardless of whether pyruvate was absent or present (Fig. 6, B). This indicates that UCP2 is mainly regulated by glutamine. We suggest that UCP2 expression increase during glucose shortage/reduced mitochondrial pyruvate entry is caused by an increase in glutamine uptake. The latter mechanism compensates for the reduced mitochondrial pyruvate oxidation. The incubation of cells at low glucose and low glutamine concentrations revealed a delayed decrease of UCP2 (Fig. 6, C) when compared to UCP2 levels during glutamine shortage and a full glucose supply (Fig. 2, B). This implies that cells first utilize glutamine to compensate for glucose shortage.

Based on the fact that UCP2 levels are strongly connected to the availability of glutamine, we assumed that higher glutamine concentrations would further upregulate UCP2. Incubation with up to 6 mM glutamine for 2 h indeed resulted in such an increase (Fig. 6, D). However, no further UCP2 increase was observed after incubation with 8 mM glutamine, suggesting that this might be the maximal capacity of glutamine usage for these cells.

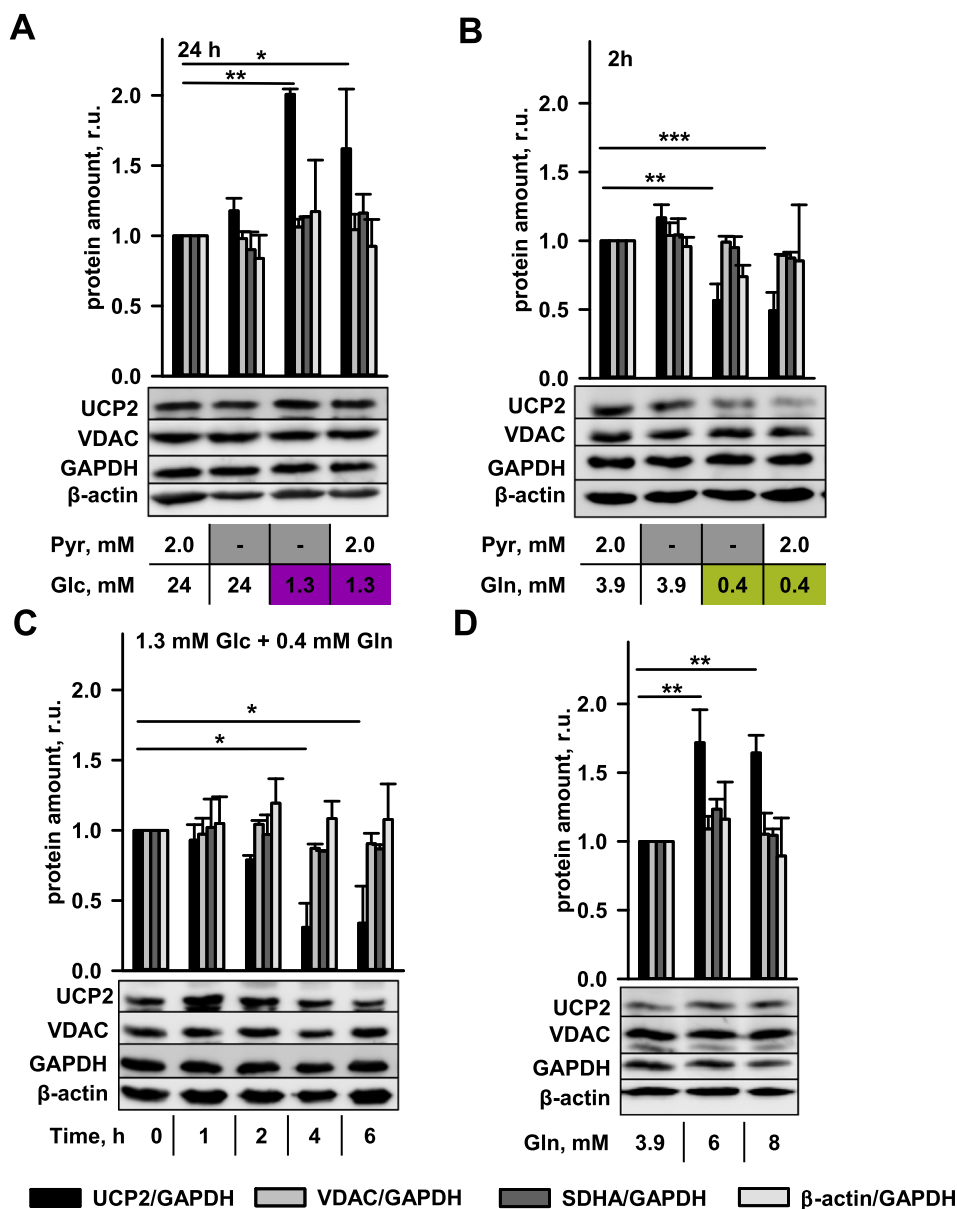


**Fig. 6.** UCP2 expression depends on the glutamine availability. Immunoblot analysis for the indicated proteins was performed on total cellular protein from N18TG2 cells. Cells were grown for stated incubation times with different concentrations of pyruvate (Pyr) and Glc (A), Pyr and Gln (B) or Glc and Gln (C). Data represent mean values ± SD for three (A, B) or two (C) independent experiments. Data are calculated as immunoblot band intensity ratios to GAPDH and normalized to the control. (D) Immunoblot analysis of N18TG2 cells after their incubation for 2 h with increased Gln concentrations. Data are presented as mean values ± SD of at least three independent experiments.

2.7. Glutamine directly regulates UCP2 at the translational level

The rapid regulation of UCP2 during nutrient shortage occurred mainly at the protein level (Figs. 1 and 2). There are two possibilities as to how cells can modulate UCP2 protein content: the regulation of protein translation [34] and protein degradation [35,36]. To detect which of both processes is mainly involved in the regulation of UCP2 protein levels by glutamine shortage, we compared UCP2 protein levels after 1 and 2 h of incubation without glutamine and/or with the protein synthesis inhibitor cycloheximide (Fig. 7, A). The shortage of glutamine or/and the addition of cycloheximide resulted in the same UCP2 decrease, indicating that UCP2 is regulated at the translational level. This supports the previous report that glutamine is essential for overcoming the translational inhibition of UCP2 [37]. The moderate increase in UCP2 protein levels during glucose shortage can be caused (i) by reduced translational inhibition due to the increased cellular amount of glutamine or (ii) an increase in protein stability due to its reduced degradation. The inhibition of UCP2 translation during glucose shortage did not prevent rapid UCP2 degradation (Fig. 7, B). The simultaneous analysis of VDAC, SDHA, GAPDH and β-actin in these

samples revealed their longer lifetimes and the singularity of UCP2 (Fig. 7, C). The reduction in UCP2 levels during glutamine shortage was swiftly recovered by addition of glutamine (Fig. 7, C, sixth column). In comparison, the addition of glutamic acid, the closest metabolite in the glutamine metabolism, was not able to recover the expression of UCP2 (Fig. 7, C; fourth column). This further supports the idea that glutamine alone is responsible for changes in UCP2 protein levels. Moreover, the addition of aspartate, described as transported substrate of UCP2 [22] and major product of mitochondrial respiration in highly proliferating cells [38] failed to recover UCP2 expression after glutamine shortage as well (Fig. 7, C; fifth column). Therefore, we concluded that glutamine only, but not the glutamine metabolites, regulates UCP2 expression.

The oncogene c-myc has been described as the main driver of glutaminolysis in cancer cells [39,40]. We found that N18TG2 cells were c-myc positive (Fig. 7, D), which indicates the c-myc-driven glutamine-addicted metabolism of these cells. However, we did not observe changes in c-myc levels under conditions that are typical for UCP2 downregulation and reduction of the metabolic activity. It contradicts to the direct involvement of c-myc in the rapid regulation of UCP2 protein levels and implies the possible dysregulation of c-myc in this

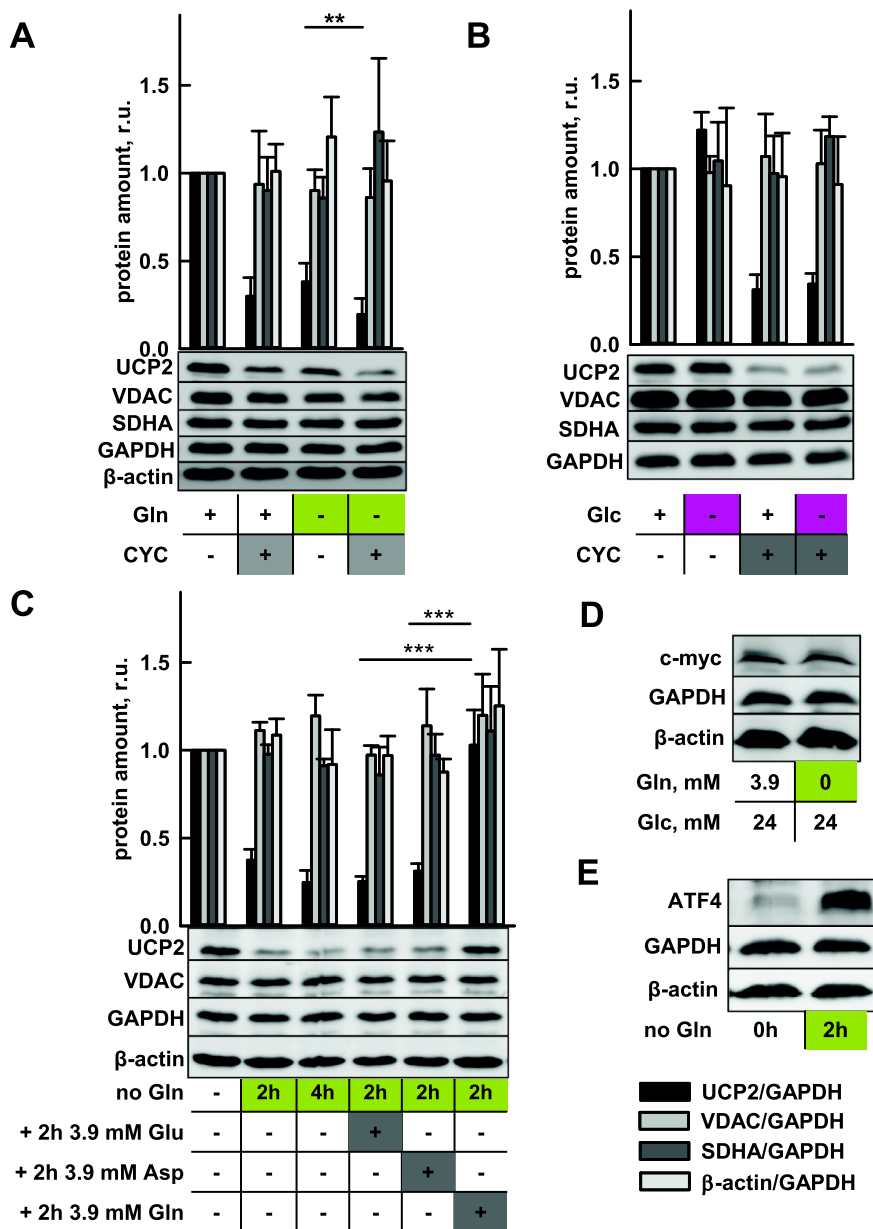


**Fig. 7.** UCP2 is directly regulated by glutamine on translational level.

Total cellular protein from N18TG2 cells was analyzed with the indicated antibodies. Cells were incubated with 10  $\mu$ g/ml cycloheximide (CYC) with or without Gln (A) or Glc (B). UCP2, VDAC, SDHA and  $\beta$ -actin band intensities are shown as a ratio to the band intensity of GAPDH and normalized to the control. The graph demonstrates the mean values  $\pm$  SD from at least three independent experiments and a representative immunoblot. (C) Recovery study was performed with N18TG2 cells after 2 h shortage of glutamine after addition 3.9 mM glutamic acid (Glu), aspartic acid (Asp) or Gln. The graph shows the quantitative analysis of three independent immunoblot analyses (mean values  $\pm$  SD). Band intensities for respective proteins were calculated as a ratio to band intensity of GAPDH and normalized to a control. Representative immunoblot analysis for c-myc (D) or ATF4 (E) was done using total cellular protein from N18TG2 cell after 2 h of Gln shortage.

cancer cell line [41].

Interestingly, we detected upregulation of the stress sensor activating transcription factor 4 (ATF4) after glutamine shortage (Fig. 7, E). ATF4 is known to help cells endure the stress of nutrient shortage [42]. Similar to UCP2, ATF4 is mainly regulated at the translational level through an upstream open reading frame (uORF) by amino acids. Our observation suggest the participation of ATF4 in the adaptation process during glutamine shortage, which shifts the cells to a more quiescent state.

### 3. Discussion

#### 3.1. UCP2 promotes glutaminolysis

Since its discovery the function of UCP2 is controversially discussed. In the present study, we provided evidence that UCP2 is employed as a fast adaptable tool to enhance glutaminolysis in rapidly proliferating cells. On the one hand, this mechanism allows cells a metabolic flexibility to endure a glucose shortage. On the other hand, the rapid

turnover of UCP2 protein enables the fast adaptation of cells to low glutamine availability and thereby prevents the consumption of glutamine as an energetic fuel, sparing it for processes that are essential for cell survival. Our study highlights a short-term effect that takes place within 1 h. It may differ from adaptation processes occurring in long-term nutrient stress application. Fig. 8 demonstrates the UCP2-driven metabolic adaptation during glucose shortage. UCP2's activity as an exporter of C4 metabolites (i.e., oxaloacetate, malate and aspartate), combined with proton-coupled phosphate import, may provide a molecular mechanism by which UCP2 supports glutaminolysis [22]. The transport of CAC intermediates out of mitochondria allows the continuous entry of glutamine-derived  $\alpha$ -ketoglutarate ( $\alpha$ KG) and thereby an increase in glutaminolysis.

In contrast, our data do not assign a role to proton transport activity of UCP2 [9,14] under conditions of the study. Although N18TG2 cells were reported to have a 30% difference in the membrane potential with and without glutamine [43] and we observed a reduced  $H^+$  leak - dependent OCR in the absence of glutamine, the missing increase in proton leak during glucose deficiency refutes the possibility that UCP2

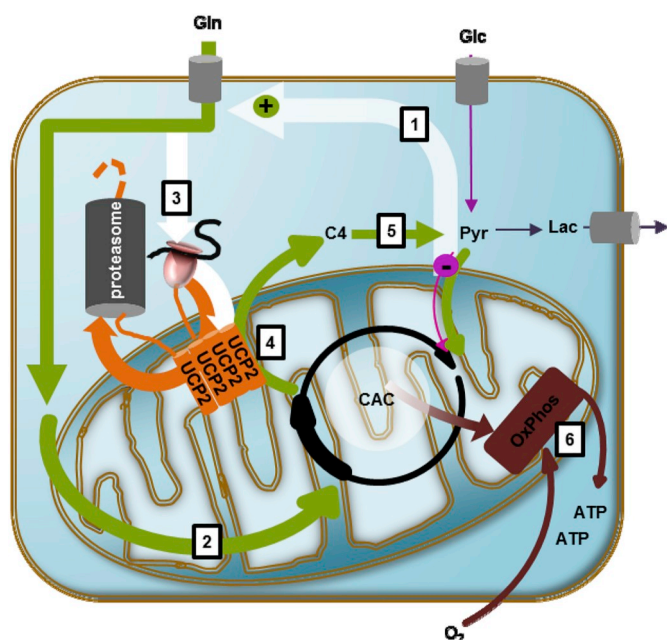


**Fig. 8.** UCP2 - supported shift to glutaminolysis during glucose shortage. The entry of pyruvate (Pyr) into the mitochondria is reduced during glucose (Glc, pink arrow) shortage (1). This induces an increase of glutamine (Gln, green arrow) uptake and usage (2) to compensate the reduced mitochondrial oxidative phosphorylation (OxPhos). The high intracellular Gln overcomes the translational regulation of UCP2 (3) yielding in a higher level of UCP2 protein despite the fast proteasomal degradation (orange arrow). With the increase of UCP2 content the export of four-carbon metabolites (C4) from the citrate acid cycle (CAC) is increased (4), which boosts the CAC filling by Gln. C4 metabolites e.g. malate (5) can be converted into Pyr to enter the mitochondria to drive the OxPhos (6). (For interpretation of the references to colour in this figure legend, the reader is referred to the web version of this article.)

acts as a proton transporter. The leak reduction might be caused by the overall energetic quiescence that affects also other mitochondrial carriers such as the proton-dependent phosphate carrier [44]. Moreover, the expression level of UCP2 in N18TG2 cells [9] is significant lower than UCP1 in brown adipose tissue [19]. Thus, its ability to effectively induce uncoupling appears doubtful. Finally, the presence of fatty acids is a *condicio sine qua non* for the protonophoric activity of UCP2 [45]. Since there is no evidence for the increase in free fatty acid amount, we can rule out a significant contribution of UCP2-mediated proton transport under the experimental conditions of this study.

Our results support the hypothesis [46] that UCP2 may have a dual function, acting as a proton and substrate transporter. A similar feature was reported for other mitochondrial carriers [47].

### 3.2. Increased glutaminolysis allows metabolic adaptation during glucose shortage

Extensive consumption of glutamine is known for rapidly proliferating cells and is a hallmark of cancer cell metabolism (s. Introduction). Glutamine can serve as an alternative substrate during glucose shortage [6,48]. The observation, that the OCR of neuroblastoma cells remained stable during glucose shortage, indicates the usage of an alternative fuel to maintain the level of oxygen consumption (Fig. 3, B). In contrast, we observed that under full nutrient supply the chemical inhibition of mitochondrial pyruvate import led to a reduction of the OCR (Fig. 5, A). This implies that glutamine recovers the reduced pyruvate oxidation during glucose shortage by pyruvate production from malate, which is known to be typical of glutaminolysis [5]. By exporting malate out of mitochondria, UCP2 may support this process. Additionally, UCP2 is upregulated parallel to the increase of

glucose and pyruvate concentrations supporting the idea of UCP2 involvement in this adaptation. The importance of UCP2 for metabolic flexibility was shown in UCP2-deficient T-cells, which were unable to survive glucose shortage [21]. Moreover, the silencing of UCP2 impaired glutamine metabolism [22,49]. The reduced import of pyruvate into mitochondria might also be a signal for this adaptation process to occur (Figs. 5, A and 6, A).

### 3.3. Glutamine acts as a signaling molecule

Our study points out that glutamine per se acts as an important signaling substance. One of its downstream targets is UCP2. We found that glutamine shortage (Fig. 2), but not the inhibition of glutaminase (Fig. 5, C) led to a faster and more pronounced reduction of UCP2 protein levels, cell metabolic activity, and cell proliferation. The addition of glutamic acid (first metabolite of glutamine metabolism) was unable to recover the reduced UCP2 protein expression in our study (Fig. 7, C). Also, other proteins that are involved in cell metabolism and proliferation were found to be regulated by glutamine but not by glutamine metabolites [50–52]. Furthermore, it has recently been shown that the reduced proliferation during glutamine deficiency was not due to the reduced metabolic degradation of glutamine but rather attributable to its role as an amino acid exchanger [53,54]. Such glutamine-regulated processes are able to alter the energetic state of the cell.

The importance of glutamine is obvious. Glutamine shortage rapidly induces a reversible lower energetic state of the cells, with a reduction of the total metabolic activity (ORC and ECAR) (Fig. 3), UCP2 protein levels (Fig. 2) and later also cell proliferation (Fig. 4). Similar cellular quiescence is known for different cells such as stem cells, fibroblasts, immune cells and cancer cells, defined as a “reversible non-proliferative state”, that protects against cellular stress caused by nutrient deprivation [55]. Glutamine is essential as a nitrogen source, for the production of nucleotides, amino acids and hexosamines, and for glutathione production. It is therefore mandatory for the proliferation and survival of each cell [56]. It was suggested that the glutamine usage for nucleotide synthesis is more important as its usage in the TCA cycle [54]. The observed effects occurred after longer treatment times (e.g., 72 h in [54]). This is in line with our observation of cell proliferation reduction, but contrasts with the fast adaptation to metabolic quiescence. Obviously, the usage of glutamine as an energetic fuel is less significant. Therefore, the fast and strong downregulation of metabolic activity (Fig. 3) and UCP2 abundance (Fig. 2) by glutamine shortage appears to be a protective mechanism. Both processes could be swiftly reversed by glutamine accessibility. In line with this, we observed a decrease of OCR within 1 h during glutamine deprivation, following by a decrease of ECAR after 4 h. This indicates a primary reduction of glutaminolysis before reducing the total metabolic activity. The dependence of N18TG2 cells on glutamine observed in the present study might be c-myc driven and reflect a special type of cancer metabolism that is known as glutamine addiction [39].

### 3.4. Rapid regulation mechanisms for UCP2 allow fast metabolic adaptation

The rapid regulation of UCP2 by glutamine shown earlier [22,37,49] and in this study is unique. UCP2 translation regulation depends on the glutamine abundance (Fig. 7). An uORF was found to inhibit the translation [37]. Only glutamine can overcome this inhibition. The best known uORF-containing translation mechanism regulates the expression of activating transcription factor 4 (ATF4). Interestingly, ATF4 is an important signaling protein that is involved in amino acid deprivation [42]. In contrast to UCP2, the absence of glutamine and amino acids induces the expression of ATF4. We detected its upregulation during glutamine shortage, when UCP2 was absent. This indicates the involvement of ATF4 in the reduction of metabolic and proliferating activity during glutamine shortage. ATF4 was found to

protect cells during short-term nutrient shortage. But it induces apoptosis and autophagy as a long-term effect [42]. The combination of this translational regulation [37], rapid UCP2 protein turnover [35] and persistently high levels of UCP2 mRNA (Fig. 2) [9,19] allows the rapid and reversible adjustment of UCP2. We found that UCP2 protein abundance in N18TG2 cells reached its peak in the presence of 6 mM glutamine. This may be different in other cancer cells, which were reported to have a UCP2 expression maximum at 1 mM glutamine [37]. This maximal expression might be directly correlated with glutaminolysis levels in the cell. This may explain the varying levels of UCP2 and even its absence in different cancer cells [26]. Importantly, glutaminolysis is not only restricted to cancer cells. It was found in other proliferating cells, such as T-cells [57], macrophages [58], stem cells [59], fibroblasts [60] and immature cardiomyocytes [61]. UCP2 expression was demonstrated in all of these cell types [9,19–21,49,62]. Nubel and colleagues showed that UCP2 expression was essential for glutamine oxidation in macrophages [49]. All this implies that UCP2 serves as a marker of high glutamine usage. The observed upregulation of UCP2 due to oxidative stress [62] may also be explained by an increased uptake of glutamine and usages of glutamine in the glutathione homeostasis [22].

Summarizing, UCP2 boosts glutaminolysis to adapt energy metabolism during glucose shortage. The rapid UCP2 expression regulation directly by glutamine enables a unique rapid glutamine usage for cell metabolism.

## 4. Experimental procedures

### 4.1. Chemicals

BPTES, UK-5099 (both Sigma-Aldrich, Inc.) and Compound 968 (Merck Inc.) were dissolved in DMSO. Etomoxir (Sigma-Aldrich, Inc.) was prepared as a water solution.

### 4.2. Cell culture

The murine neuroblastoma cell line was cultivated as described in [9]. For immunoblotting and quantitative PCR analysis, cells were seeded in pre-coated 6-well plates (Greiner, Bio One, Inc.) and grown in control media, DMEM with high glucose (24 mM), supplemented with 2 mM pyruvate (both from Sigma-Aldrich Austria), 3.9 mM glutamine (Thermo Fisher Scientific, Inc.) and B27 serum-free supplement (Thermo Fisher Scientific, Inc.) for 48 h before harvesting. For the nutrient concentration-dependent analysis, the media were changed after one wash step, and cells were incubated until the required time point within a total growth time of 48 h. For each independent experiment, another passage of N18TG2 cells was seeded and maintained on a control cell plate, which was treated with an equal wash step but grown in full media.

### 4.3. Protein isolation and quantitative immunoblot analysis

Protein isolation from cells and Western blot analysis were performed as described in [9]. In brief, the cells were washed in PBS, collected in RIPA-buffer with 1:50 protease inhibitor cocktail, and sonicated. Total cellular protein was isolated after centrifugation and quantitatively determined using a BCA kit (Thermo Fisher Scientific, Inc.).

We loaded 20 and 50 µg total cellular protein per lane for UCP2 and signaling protein immunoblot analyses respectively. We used antibodies against UCP2, VDAC, SDHA, Hsp60, GAPDH, and β-actin evaluated previously [9,19] (Supplementary Materials, Fig. S1 and S2). Antibodies against ATF4 protein (Cell Signaling Technology, Netherlands) and against c-myc (Santa Cruz, SZABO-SCANDIC, Austria) were diluted 1:1000 and 1:500, respectively. Immunoreactions were revealed by luminescence using a secondary antibody against rabbit or

mouse antibodies linked with horseradish peroxidase (GE Healthcare, Austria) and ECL Western Blotting reagent (Bio-Rad, Austria). The intensity of the bands was detected using the ChemiDoc-It 600 Imaging System (UVP, UK) and measured with Launch Vision Works LS software (UVP, UK). The immunoblot intensities of the different detected proteins were calculated as a ratio relative to the intensity of GAPDH. All obtained values from one experiment were normalized to ratio values of its controls. For each independent experiment, two immunoblots were performed to exclude possible incorrect interpretations caused by artefacts of the immunoblotting method.

### 4.4. RNA isolation and quantitative PCR analysis

Total RNA was isolated from N18TG2 cells using the RNeasy Mini Kit (QIAGEN, Inc.) according to the manufacturer's instructions. cDNA was produced using the high-capacity cDNA reverse transcription kit (Applied Biosystems, Austria) according to the manufacturer's instructions. Using the ViiA™ 7 Real-Time PCR System (Applied Biosystems, Austria), ct values for *ucp2* and *gapdh* in each sample were determined in parallel using TaqMan® Gene Expression Assay UCP2 Mm00627598\_m1 FAM-MGB, TaqMan Gene expression assay GAPDH Mm99999915\_g1 VIC-MGB\_PL, and the QuantiFast Multiplex PCR kit (QIAGEN, Inc.). *ucp2* was calculated as a ratio relative to *gapdh*, and all values were normalized to the control.

### 4.5. Determination of the oxygen consumption rate (OCR) and extracellular acidification rate (ECAR)

N18TG2 cells were seeded on poly-D-lysine (Sigma) - coated Seahorse 96XFe plates (Agilent, Inc.) for approximately 16 h before the analysis with 20,000 cells per well in the control media. For the nutrient shortage experiments, the whole plate was washed with DMEM and then filled with new media (control or nutrient shortage media). One hour before the experiment, the media were changed to unbuffered XF base media (Agilent) containing the indicated amounts of glucose and glutamine, 2 mM pyruvate, and B27. The OCR and ECAR were determined in parallel using an XFe96 extracellular flux analyzer (Seahorse Bioscience). The compounds of the Seahorse XF Cell Mito Stress Test Kit (Agilent, Inc.) were applied according to the manufacturer's instructions at the adjusted concentrations (1 µM oligomycin, 1.2 µM FCCP, 1 µM rotenone and 1 µM antimycin A). Each independent experiment was performed on a new plate. Wells displaying a deviation in the cell layer were not further analyzed. Due to dehydration processes, the wells at the edge of the plate were not included in the calculation. The minimal number of wells per condition for each experiment was five (for the basal measurements) and three (Mito Stress Test and mitochondrial nutrient usage inhibition analysis). The OCR and ECAR were normalized to the mean of the technical replicates of the respective control experiment. Due to the varying number of technical replicates of different experiments we employed a random number generator to create 1000 values for each control and each condition to count in the calculation of the mean and standard deviation equally for all independent experiments. This allowed us to include the variation within each independent experiment in the overall analysis.

### 4.6. Growth rate assay

Cells were plated at a concentration of 10<sup>5</sup> cells/ml in 6-well plates and cultivated in different media (control, low glucose, and low glutamine medium). After 24, 48, and 72 h of cultivation, N18TG2 cells were resuspended and 20 µl of suspension was diluted in 380 µl trypan blue solution (4 µg trypan blue in 1 ml 0.9% NaCl). Cell number was calculated using a Neubauer counting chamber.

#### 4.7. Glutamine consumption

For glutamic acid/glutamine determination, a bioluminescent assay was used following manufacturer's description (Promega, Mannheim, Germany). In brief, cells ( $10^5$  cells/ml) were seeded on plates for 24 h before treatment with full- and low-glucose media for another 4 h. Total glutamine and glutamic acid levels were determined in the supernatant before and after the 4-h incubation time and subtracted to calculate consumption. Glutamic acid concentration has been subtracted. The data were normalized to the total protein concentration per well.

#### 4.8. Statistical analysis

Significance was determined using the one-way ANOVA and *t*-test against the control and pairwise. Significance is indicated as \*  $p < 0.05$ ; \*\*  $p < 0.01$ ; \*\*\*  $p < 0.001$ .

#### Transparency document

The Transparency document associated with this article can be found, in online version.

#### Acknowledgements

We thank Sarah Bardakji, Christopher Krewenka, and Sarah Rosenthaler for the great technical support. We acknowledge Soleman Sasgary and Günther Schauberg for valuable scientific discussions.

EP and AR are grateful to BMBS COST Action BM1406 (IONCHANIMMUNRESPON) for the scientific exchange and cooperation.

This work was partly supported by Austrian Science Fund (FWF, P25357-820 to EP).

#### Declaration of interests

The authors declare no competing interests.

#### Appendix A. Supplementary data

Supplementary data to this article can be found online at <https://doi.org/10.1016/j.bbabo.2019.03.006>.

#### References

- [1] S.Y. Lunt, M.G. Vander Heiden, Aerobic glycolysis: meeting the metabolic requirements of cell proliferation, *Annu. Rev. Cell Dev. Biol.* 27 (2011) 441–464.
- [2] P.S. Ward, C.B. Thompson, Metabolic reprogramming: a cancer hallmark even Warburg did not anticipate, *Cancer Cell* 21 (2012) 297–308.
- [3] N.J. MacIver, R.D. Michalek, J.C. Rathmell, Metabolic regulation of T lymphocytes, *Annu. Rev. Immunol.* 31 (2013) 259–283.
- [4] L. Jin, G.N. Alesi, S. Kang, Glutaminolysis as a target for cancer therapy, *Oncogene* 35 (2016) 3619–3625.
- [5] R.J. DeBerardinis, A. Mancuso, E. Daikhin, I. Nissim, M. Yudkoff, S. Wehrli, C.B. Thompson, Beyond aerobic glycolysis: transformed cells can engage in glutamine metabolism that exceeds the requirement for protein and nucleotide synthesis, *Proc. Natl. Acad. Sci. U. S. A.* 104 (2007) 19345–19350.
- [6] C. Yang, B. Ko, C.T. Hensley, L. Jiang, A.T. Wasti, J. Kim, J. Sudderth, M.A. Calvaruso, L. Lumata, M. Mitsche, J. Rutter, M.E. Merritt, R.J. DeBerardinis, Glutamine oxidation maintains the TCA cycle and cell survival during impaired mitochondrial pyruvate transport, *Mol. Cell* 56 (2014) 414–424.
- [7] J.R. Mayers, M.G. Vander Heiden, Famine versus feast: understanding the metabolism of tumors in vivo, *Trends Biochem. Sci.* 40 (2015) 130–140.
- [8] R.J. DeBerardinis, N.S. Chandel, Fundamentals of cancer metabolism, *Sci. Adv.* 2 (2016) e1600200.
- [9] A. Rupprecht, D. Sittner, A. Smorodchenko, K.E. Hulse, J. Goyn, R. Moldzio, A.E. Seiler, A.U. Brauer, E.E. Pohl, Uncoupling protein 2 and 4 expression pattern during stem cell differentiation provides new insight into their putative function, *PLoS One* 9 (2014) e88474.
- [10] P. Esteves, C. Pecqueur, M.C. Alves-Guerra, UCP2 induces metabolic reprogramming to inhibit proliferation of cancer cells, *Mol. Cell Oncol.* 2 (2015) e975024.
- [11] C.T. Madreiter-Sokolowski, B. Gyorffy, C. Klec, A.A. Sokolowski, R. Rost, M. Waldeck-Weiermair, R. Malli, W.F. Graier, UCP2 and PRMT1 are key prognostic markers for lung carcinoma patients, *Oncotarget* 8 (2017) 80278–80285.
- [12] E. Klotzsch, A. Smorodchenko, L. Lofler, R. Moldzio, E. Parkinson, G.J. Schutz, E.E. Pohl, Superresolution microscopy reveals spatial separation of UCP4 and F0F1-ATP synthase in neuronal mitochondria, *Proc. Natl. Acad. Sci. U. S. A.* 112 (2015) 130–135.
- [13] M. Jaburek, K.D. Garlid, Reconstitution of recombinant uncoupling proteins: UCP1, -2, and -3 have similar affinities for ATP and are unaffected by coenzyme Q10, *J. Biol. Chem.* 278 (2003) 25825–25831.
- [14] V. Beck, M. Jaburek, T. Demina, A. Rupprecht, R.K. Porter, P. Jezek, E.E. Pohl, Polyunsaturated fatty acids activate human uncoupling proteins 1 and 2 in planar lipid bilayers, *FASEB J.* 21 (2007) 1137–1144.
- [15] G. Macher, M. Koehler, A. Rupprecht, J. Kreiter, P. Hinterdorfer, E.E. Pohl, Inhibition of mitochondrial UCP1 and UCP3 by purine nucleotides and phosphate, *Biochim. Biophys. Acta* 1860 (2018) 664–672.
- [16] R.J. Mailloux, M.E. Harper, Uncoupling proteins and the control of mitochondrial reactive oxygen species production, *Free Radic. Biol. Med.* 51 (2011) 1106–1115.
- [17] M.D. Brand, C. Affourtit, T.C. Esteves, K. Green, A.J. Lambert, S. Miwa, J.L. Pakay, N. Parker, Mitochondrial superoxide: production, biological effects, and activation of uncoupling proteins, *Free Radic. Biol. Med.* 37 (2004) 755–767.
- [18] S. Krauss, C.Y. Zhang, B.B. Lowell, The mitochondrial uncoupling-protein homologues, *Nat. Rev. Mol. Cell Biol.* 6 (2005) 248–261.
- [19] A. Rupprecht, A.U. Brauer, A. Smorodchenko, J. Goyn, K.E. Hulse, I.G. Shabalina, C. Infante-Duarte, E.E. Pohl, Quantification of uncoupling protein 2 reveals its main expression in immune cells and selective up-regulation during T-cell proliferation, *PLoS One* 7 (2012) e41406.
- [20] J. Zhang, I. Khvorostov, J.S. Hong, Y. Oktay, L. Vergnes, E. Nuebel, P.N. Wahjudi, K. Setoguchi, G. Wang, A. Do, H.J. Jung, J.M. McCaffery, I.J. Kurland, K. Reue, W.N. Lee, C.M. Koehler, M.A. Teitell, UCP2 regulates energy metabolism and differentiation potential of human pluripotent stem cells, *EMBO J.* 30 (2011) 4860–4873.
- [21] C. Pecqueur, T. Bui, C. Gelly, J. Hauchard, C. Barbot, F. Bouillaud, D. Ricquier, B. Miroux, C.B. Thompson, Uncoupling protein-2 controls proliferation by promoting fatty acid oxidation and limiting glycolysis-derived pyruvate utilization, *FASEB J.* 22 (2008) 9–18.
- [22] A. Vozza, G. Parisi, F. De Leonardi, F.M. Lasorsa, A. Castegna, D. Amorese, R. Marmo, V.M. Calcagnile, L. Palmieri, D. Ricquier, E. Paradies, P. Scarcia, F. Palmieri, F. Bouillaud, G. Fiermonte, UCP2 transports C4 metabolites out of mitochondria, regulating glucose and glutamine oxidation, *Proc. Natl. Acad. Sci. U. S. A.* 111 (2014) 960–965.
- [23] M.E. Harper, A. Antoniou, E. Villalobos-Menuy, A. Russo, R. Trauger, M. Vendemio, A. George, R. Bartholomew, D. Carlo, A. Shaikh, J. Kupperman, E.W. Newell, I.A. Bespalov, S.S. Wallace, Y. Liu, J.R. Rogers, G.L. Gibbs, J.L. Leahy, R.E. Camley, R. Melamed, M.K. Newell, Characterization of a novel metabolic strategy used by drug-resistant tumor cells, *FASEB J.* 16 (2002) 1550–1557.
- [24] I. Samudio, M. Fiegl, T. McQueen, K. Clise-Dwyer, M. Andreeff, The Warburg effect in leukemia-stroma cocultures is mediated by mitochondrial uncoupling associated with uncoupling protein 2 activation, *Cancer Res.* 68 (2008) 5198–5205.
- [25] Z. Derdak, N.M. Mark, G. Beldi, S.C. Robson, J.R. Wands, G. Baffy, The mitochondrial uncoupling protein-2 promotes chemoresistance in cancer cells, *Cancer Res.* 68 (2008) 2813–2819.
- [26] P. Esteves, C. Pecqueur, C. Ransy, C. Esnous, V. Lenoir, F. Bouillaud, A.L. Bulteau, A. Lombes, C. Prip-Buus, D. Ricquier, M.C. Alves-Guerra, Mitochondrial retrograde signaling mediated by UCP2 inhibits cancer cell proliferation and tumorigenesis, *Cancer Res.* 74 (2014) 3971–3982.
- [27] S. Rousset, J. Mozo, G. Dujardin, Y. Emre, S. Masscheleyn, D. Ricquier, A.M. Cassard-Doulcier, UCP2 is a mitochondrial transporter with an unusual very short half-life, *FEBS Lett.* 581 (2007) 479–482.
- [28] H. Eagle, V.I. Oyama, M. Levy, C.L. Horton, R. Fleischman, The growth response of mammalian cells in tissue culture to L-glutamine and L-glutamic acid, *J. Biol. Chem.* 218 (1956) 607–616.
- [29] F. Buttgerit, M.D. Brand, A hierarchy of ATP-consuming processes in mammalian cells, *Biochem. J.* 312 (Pt 1) (1995) 163–167.
- [30] M.J. Lukey, K.F. Wilson, R.A. Cerione, Therapeutic strategies impacting cancer cell glutamine metabolism, *Future Med. Chem.* 5 (2013) 1685–1700.
- [31] R.V. Duran, W. Opplinger, A.M. Robitaille, L. Heiserich, R. Skendaj, E. Gottlieb, M.N. Hall, Glutaminolysis activates rag-mTORC1 signaling, *Mol. Cell* 47 (2012) 349–358.
- [32] X. Wang, C.G. Proud, The mTOR pathway in the control of protein synthesis, *Physiology (Bethesda)* 21 (2006) 362–369.
- [33] M. Morita, S.P. Gravel, L. Hulea, O. Larsson, M. Pollak, J. St-Pierre, I. Topisirovic, mTOR coordinates protein synthesis, mitochondrial activity and proliferation, *Cell Cycle* 14 (2015) 473–480.
- [34] C. Hurtaud, C. Gelly, F. Bouillaud, C. Levi-Meyruis, Translation control of UCP2 synthesis by the upstream open reading frame, *Cell. Mol. Life Sci.* 63 (2006) 1780–1789.
- [35] V. Azzu, C. Affourtit, E.P. Breen, N. Parker, M.D. Brand, Dynamic regulation of uncoupling protein 2 content in INS-1E insulinoma cells, *Biochim. Biophys. Acta* 1777 (2008) 1378–1383.
- [36] V. Azzu, M.D. Brand, Degradation of an intramitochondrial protein by the cytosolic proteasome, *J. Cell Sci.* 123 (2010) 578–585.
- [37] C. Hurtaud, C. Gelly, Z. Chen, C. Levi-Meyruis, F. Bouillaud, Glutamine stimulates translation of uncoupling protein 2mRNA, *Cell. Mol. Life Sci.* 64 (2007) 1853–1860.
- [38] L.B. Sullivan, D.Y. Gui, A.M. Hosios, L.N. Bush, E. Freinkman, M.G. Vander Heiden, Supporting aspartate biosynthesis is an essential function of respiration in proliferating cells, *Cell* 162 (2015) 552–563.
- [39] D.R. Wise, R.J. DeBerardinis, A. Mancuso, N. Sayed, X.Y. Zhang, H.K. Pfeiffer,

- I. Nissim, E. Daikhin, M. Yudkoff, S.B. McMahon, C.B. Thompson, Myc regulates a transcriptional program that stimulates mitochondrial glutaminolysis and leads to glutamine addiction, *Proc. Natl. Acad. Sci. U. S. A.* 105 (2008) 18782–18787.
- [40] Z.E. Stine, Z.E. Walton, B.J. Altman, A.L. Hsieh, C.V. Dang, MYC, metabolism, and Cancer, *Cancer Discov.* 5 (2015) 1024–1039.
- [41] M. Kalkat, J. De Melo, K.A. Hickman, C. Lourenco, C. Redel, D. Resetca, A. Tamachi, W.B. Tu, L.Z. Penn, MYC deregulation in primary human cancers, *Genes (Basel)*, 8 (2017).
- [42] I.M.N. Wortel, L.T. van der Meer, M.S. Kilberg, F.N. van Leeuwen, Surviving stress: modulation of ATF4-mediated stress responses in normal and malignant cells, *Trends Endocrinol. Metab.* 28 (2017) 794–806.
- [43] L. Zimmermann, R. Moldzio, K. Vazdar, C. Krewenka, E.E. Pohl, Nutrient deprivation in neuroblastoma cells alters 4-hydroxynonenal-induced stress response, *Oncotarget* 8 (2017) 8173–8188.
- [44] F. Palmieri, The mitochondrial transporter family SLC25: identification, properties and physiopathology, *Mol. Asp. Med.* 34 (2013) 465–484.
- [45] A. Rupprecht, E.A. Sokolenko, V. Beck, O. Ninnemann, M. Jaburek, T. Trimbuch, S.S. Klshin, P. Jezek, V.P. Skulachev, E.E. Pohl, Role of the transmembrane potential in the membrane proton leak, *Biophys. J.* 98 (2010) 1503–1511.
- [46] F. Criscuolo, J. Mozo, C. Hurtaud, T. Nubel, F. Bouillaud, UCP2, UCP3, avUCP, what do they do when proton transport is not stimulated? Possible relevance to pyruvate and glutamine metabolism, *Biochim. Biophys. Acta* 1757 (2006) 1284–1291.
- [47] A.Y. Andreyev, T.O. Bondareva, V.I. Dedukhova, E.N. Mokhova, V.P. Skulachev, L.M. Tsofina, N.I. Volkov, T.V. Vygodina, The ATP/ADP-antiporter is involved in the uncoupling effect of fatty acids on mitochondria, *Eur. J. Biochem.* 182 (1989) 585–592.
- [48] L. Ma, Y. Tao, A. Duran, V. Llado, A. Galvez, J.F. Barger, E.A. Castilla, J. Chen, T. Yajima, A. Porollo, M. Medvedovic, L.M. Brill, D.R. Plas, S.J. Riedl, M. Leitges, M.T. Diaz-Meco, A.D. Richardson, J. Moscat, Control of nutrient stress-induced metabolic reprogramming by PKC $\zeta$  in tumorigenesis, *Cell* 152 (2013) 599–611.
- [49] T. Nubel, Y. Emre, D. Rabier, B. Chadeaux, D. Ricquier, F. Bouillaud, Modified glutamine catabolism in macrophages of Ucp2 knock-out mice, *Biochim. Biophys. Acta* 1777 (2008) 48–54.
- [50] A. Cacace, M. Sboarina, T. Vazeille, P. Sonveaux, Glutamine activates STAT3 to control cancer cell proliferation independently of glutamine metabolism, *Oncogene* 36 (2017) 2074–2084.
- [51] M. Corless, A. Kiely, N.H. McClenaghan, P.R. Flatt, P. Newsholme, Glutamine regulates expression of key transcription factor, signal transduction, metabolic gene, and protein expression in a clonal pancreatic  $\beta$ -cell line, *J. Endocrinol.* 190 (2006) 719–727.
- [52] H. Xue, D. Slavov, P.E. Wischmeyer, Glutamine-mediated dual regulation of heat shock transcription factor-1 activation and expression, *J. Biol. Chem.* 287 (2012) 40400–40413.
- [53] A.S. Krall, S. Xu, T.G. Graeber, D. Braas, H.R. Christofk, Asparagine promotes cancer cell proliferation through use as an amino acid exchange factor, *Nat. Commun.* 7 (2016) 11457.
- [54] S. Tardito, A. Oudin, S.U. Ahmed, F. Fack, O. Keunen, L. Zheng, H. Miletic, P.O. Sakariassen, A. Weinstock, A. Wagner, S.L. Lindsay, A.K. Hock, S.C. Barnett, E. Ruppin, S.H. Morkve, M. Lund-Johansen, A.J. Chalmers, R. Bjerkvig, S.P. Nicloul, E. Gottlieb, Glutamine synthetase activity fuels nucleotide biosynthesis and supports growth of glutamine-restricted glioblastoma, *Nat. Cell Biol.* 17 (2015) 1556–1568.
- [55] G. Yao, Modelling mammalian cellular quiescence, *Interface Focus* 4 (2014) 20130074.
- [56] R.J. DeBerardinis, T. Cheng, Q's next: the diverse functions of glutamine in metabolism, cell biology and cancer, *Oncogene* 29 (2010) 313–324.
- [57] R. Wang, C.P. Dillon, L.Z. Shi, S. Milasta, R. Carter, D. Finkelstein, L.L. McCormick, P. Fitzgerald, H. Chi, J. Munger, D.R. Green, The transcription factor Myc controls metabolic reprogramming upon T lymphocyte activation, *Immunity* 35 (2011) 871–882.
- [58] P.S. Liu, H. Wang, X. Li, T. Chao, T. Teav, S. Christen, G. Di Conza, W.C. Cheng, C.H. Chou, M. Vavakova, C. Muret, K. Debackere, M. Mazzone, H.D. Huang, S.M. Fendt, J. Ivanisevic, P.C. Ho, Alpha-ketoglutarate orchestrates macrophage activation through metabolic and epigenetic reprogramming, *Nat. Immunol.* 18 (2017) 985–994.
- [59] J.G. Lees, D.K. Gardner, A.J. Harvey, Pluripotent stem cell metabolism and mitochondria: beyond ATP, *Stem Cells Int.* 2017 (2017) 2874283.
- [60] C. Wolfrom, N. Kadhon, G. Polini, J. Poggi, N. Moatti, M. Gautier, Glutamine dependency of human skin fibroblasts: modulation by hexoses, *Exp. Cell Res.* 183 (1989) 303–318.
- [61] J.K. Salabei, P.K. Lorkiewicz, C.R. Holden, Q. Li, K.U. Hong, R. Bolli, A. Bhatnagar, B.G. Hill, Glutamine regulates cardiac progenitor cell metabolism and proliferation, *Stem Cells* 33 (2015) 2613–2627.
- [62] C. Pecqueur, M.C. Alves-Guerra, C. Gelly, C. Levi-Meyrueis, E. Couplan, S. Collins, D. Ricquier, F. Bouillaud, B. Miroux, Uncoupling protein 2, in vivo distribution, induction upon oxidative stress, and evidence for translational regulation, *J. Biol. Chem.* 276 (2001) 8705–8712.